Mixed-state properties of superconducting MgB_2 single crystals

M. Zehetmayer,[1,*] M. Eisterer,[1] J. Jun,[2] S. M. Kazakov,[2] J. Karpinski,[2] A. Wisniewski,[3] and H. W. Weber[1]
[1] *Atominstitut der Österreichischen Universitäten, A-1020 Vienna, Austria*
[2] *Solid State Physics Laboratory, ETH, CH-8093 Zurich, Switzerland*
[3] *Institute of Physics, Polish Academy of Sciences, PL-02-668 Warsaw, Poland*
(Received 26 March 2002; published 8 August 2002)

We report on measurements of the magnetic moment in superconducting MgB_2 single crystals. We find $\mu_0 H_{c2}^c(0)=3.2$ T, $\mu_0 H_{c2}^{ab}(0)=14.5$ T, $\gamma=4.6$, $\mu_0 H_c(0)=0.28$ T, and $\kappa(T_c)=4.7$. The standard Ginzburg-Landau and London model relations lead to a consistent data set and indicate that MgB_2 is a clean limit superconductor of intermediate coupling strength with very pronounced anisotropy effects.

DOI: 10.1103/PhysRevB.66.052505 PACS number(s): 74.25.Ha, 74.60.Ec, 74.70.Ad

The recent discovery of superconductivity in MgB_2 (Ref. 1) has attracted a lot of attention. Especially the rather high transition temperature of nearly 40 K in such a simple compound is of interest for applications, but also for an analysis of the physical mechanism leading to superconductivity. Several experiments indicate a phonon mediated *s*-wave BCS mechanism.[2,3] Different models are proposed to explain the particular properties of MgB_2.[4,5] Their correctness has to be checked by experiments, but only a few results are available on single crystals.[6–12]

We report on magnetization measurements on single crystalline MgB_2 in magnetic fields applied parallel and perpendicular to the uniaxial crystallographic ($\equiv c$) axis. A detailed evaluation allows us to obtain the temperature dependence of the most important reversible mixed-state parameters, such as the critical magnetic fields, the characteristic lengths, the Ginzburg-Landau (GL) parameter, and the anisotropy. We will show that MgB_2 is a clean limit superconductor of intermediate coupling strength with very pronounced anisotropy effects.

Several single crystals of MgB_2 were grown using high-pressure cubic anvils. Details of the process will be published elsewhere.[13] Two crystals (sample A: $a\times b\times c\cong 660\times 570\times 21$ μm^3; sample B: $a\times b\times c\cong 600\times 384\times 54$ μm^3) were investigated by magnetic methods. The transition temperature (T_c) of each sample was obtained from the ac susceptibility measured in a 1-T quantum interference device (SQUID) magnetometer. Sample A shows an onset of T_c at 38 K and a rather broad transition of about 1 K. A linear fit of $H_{c2}^c(T)$ near T_c indicates a "bulk transition temperature" of 37.5 K [see inset of Fig. 1(a)]. In sample B we find $T_c=38.3$ K, $\Delta T_c=0.3$ K, and a "bulk T_c" of 38.2 K. A simple analysis[14] of the slope of the magnetic moment after reversing the applied field demonstrates that the size of the domain, in which the supercurrents flow without impedance, is identical to the sample size. Furthermore, a comparison of the calculated and the measured magnetization in the Meissner regime indicates a superconducting volume fraction of about 100%. The further evaluation of the mixed-state parameters did not show significant differences between these two crystals.

The measurements of the magnetic moment were carried out in an 1-T and in an 8-T (SHE) SQUID magnetometer (for details, cf. Ref. 15). Figure 1(a) shows the upper critical field of MgB_2 for applied fields $H_a\|c$ (H_{c2}^c) and $H_a\|ab$ (H_{c2}^{ab}). $H_{c2}(T)$ is determined either from the onset of the superconducting signal in the $m(T)$ curve "$T_c(H_a)$" or from the disappearance of the superconducting signal in the $m(H_a)$ curve. The same results were obtained by both methods. H_{c2}^{ab} could be evaluated directly only below 8 T ($T>21$ K in this case). At lower temperatures the London theory for the reversible magnetic moment m_r, i.e., $m_r\propto\ln(H_{c2}/H_a)$, was used for the sake of simplicity to extrapolate the experimental m_r data to zero. The very small magnetic moment in higher fields and the logarithmic behavior lead to rather large uncertainties in the evaluation, which are indicated by error bars in Fig. 1(a).

To obtain $H_{c2}^c(0)$, the data were fitted to the function $H_{c2}(t)=H_{c2}(0)(1-t^\alpha)^\beta$ with $\mu_0 H_{c2}^c(0)=3.18$ T [$t=T/T_c$, T_c denotes the bulk transition temperature; α, β, and $H_{c2}(0)$ are fit parameters]. The initial slope of the upper critical field ($k=\mu_0[\partial H_{c2}/\partial T]_{T_c}$) is found to be -0.112 T/K near T_c, thus $\mu_0 H_{c2}^c(0)/(kT_c)=-0.75$. This is close to the weak-coupling BCS result ($\cong -0.73$ in the clean limit, -0.69 would correspond to the dirty limit[16]). k is not very sensitive to the coupling strength and the above result, -0.75, is actually close to that of the strong-coupling superconductor Pb,[17] of course without considering anisotropy effects.[4,18] If we apply the same procedure to $H_a\|ab$, we obtain $\mu_0 H_{c2}^{ab}(0)=15$ T. However, the slope was determined in this case from the linear region above 1 T ($k=-0.55$ T/K) and the corresponding extrapolated "T_c" of 36.1 K, because a strong positive curvature of $H_{c2}^{ab}(T)$ is observed in the vicinity of T_c [cf. the inset of Fig. 1(a)], which represents a well-known feature of anisotropic superconductors, e.g., of the high T_c's, but also of conventional superconductors, such as Nb.[19] The Fermi surface and the electron phonon coupling are usually held responsible for these anisotropic properties. According to Ref. 18, the high-temperature end of $H_{c2}^{ab}(T)$ can be obtained by an anisotropic Fermi velocity, but not by the coupling alone. A similar model could possibly apply in the case of MgB_2, but alternative theories are also under discussion. For example, it was shown that both, the two-band[5] and the anisotropic gap model,[20] can qualitatively describe the positive curvature near T_c.

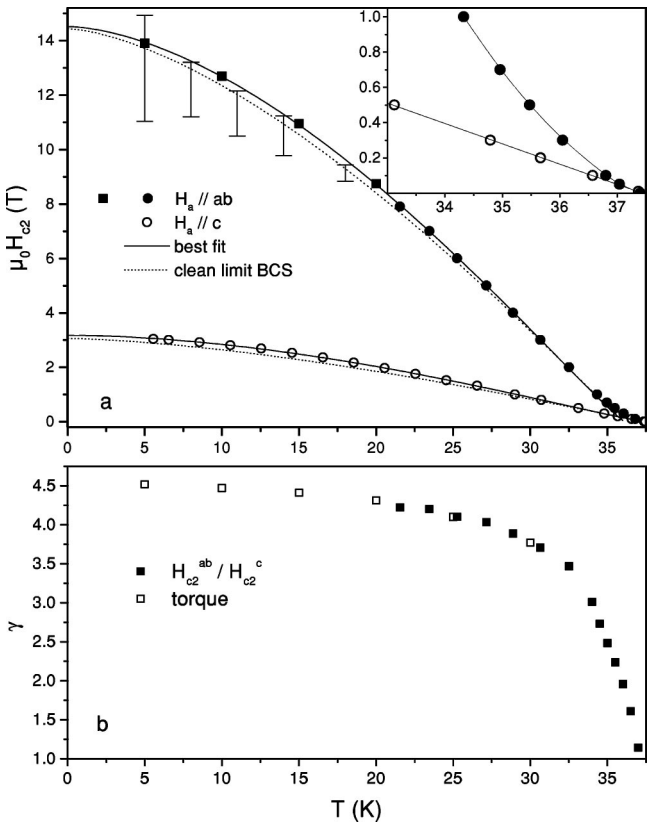

FIG. 1. (a) Upper critical field for $H_a \| c$ (H_{c2}^c) and $H_a \| ab$ (H_{c2}^{ab}). H_{c2}^{ab} is obtained from (i) a direct evaluation of $m(T)$ for $T > 21$ K (solid circles) and (ii) $H_{c2}^{ab} = \gamma H_{c2}^c$ for $T < 21$ K (solid squares). The error bars indicate the extrapolation uncertainties of the reversible moments measured up to 8 T. The BCS curves according to Ref. 16 are fitted to the experimental slope of H_{c2} near T_c. (b) Anisotropy from SQUID (H_{c2}^{ab}/H_{c2}^c) and torque measurements.

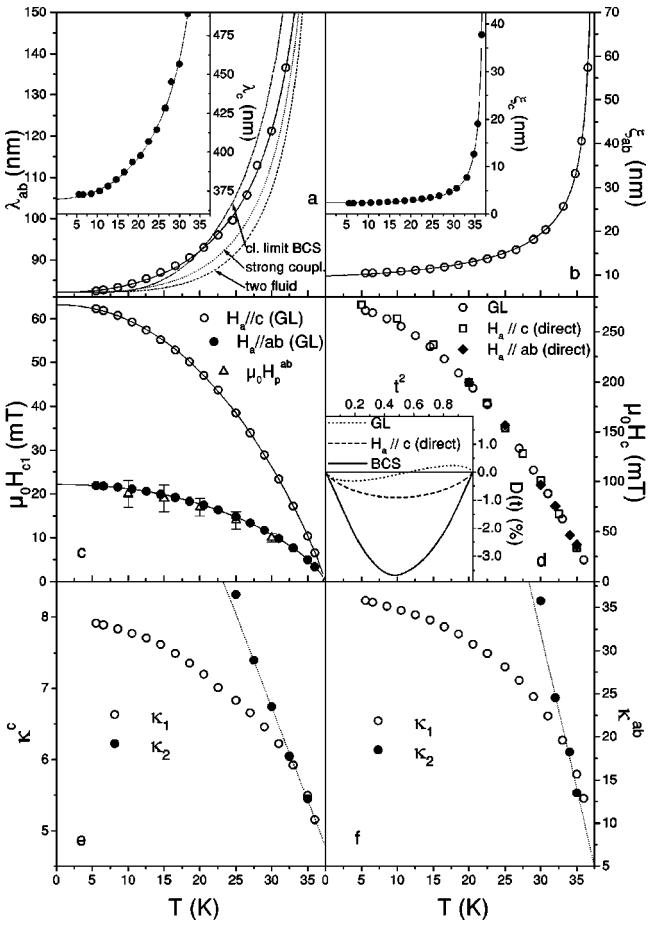

FIG. 2. Temperature dependence of (a) the magnetic penetration depths, (b) the coherence lengths, (c) the lower critical fields from the GL evaluation and the trapped magnetic moment measurements, and (d) the thermodynamic critical field and the deviation function (inset) and (e), (f) the GL parameters of MgB_2.

The upper critical-field anisotropy $\gamma = H_{c2}^{ab}/H_{c2}^c$ is shown in Fig. 1(b) (full squares). It increases from about 1 near T_c to 4.2 at 22 K, in qualitative agreement with previous results.[10–12] The open squares refer to results from torque measurements taken in a 9-T (quantum design) PPMS (physical properties measurement system) system. In this case, the angular dependence of the reversible torque is fitted to the anisotropic London theory with three fit parameters γ, H_{c2}^c, and λ_{ab} (cf. Ref. 21). The excellent agreement of the latter two parameters with results from the SQUID measurements shows the high reliability of the evaluation. Note that the torque method does not lead to the anisotropy of the upper critical field, but rather to that of the magnetic penetration depth (λ), which can, in general, deviate from H_{c2}^{ab}/H_{c2}^c. In MgB_2, both seem to be the same, at least for $T \leqslant 30$ K. The torque indicates a small increase of γ from 4.3 at 20 K to about 4.5 at 5 K leading to $\gamma(0) \cong 4.55$. However, we cannot exclude some small systematic errors in the evaluation because of the following reasons. (i) Most of the recorded torque data refer to the irreversible regime. Therefore, the reversible signal (τ) has to be calculated from the irreversible branches at increasing (τ_+) and decreasing (τ_-) angles ($\tau = [\tau_+ + \tau_-]/2$). The difference between the two branches is rather small, but grows at lower temperatures. (ii) The angular dependence of the background signal varies with temperature and cannot be determined exactly from measurements without a sample. However, different data sets for the background do not change γ at 5 K significantly. Furthermore, the torque data were evaluated at several magnetic fields (0.5–2 T), which would change possible errors due to the irreveresibility, but the differences in γ were very small (2%). Based on the excellent agreement between the SQUID and the torque data in the overlapping temperature range, we assume that $\lambda_c/\lambda_{ab} = H_{c2}^{ab}/H_{c2}^c$ for $T < 21$ K, which allows us to calculate H_{c2}^{ab} in this temperature range [cf. the solid squares for H_{c2}^{ab} at $T < 21$ K in Fig. 1(a)]. This leads to $H_{c2}^{ab}(0) = 14.5$ T. A temperature-dependent anisotropy can be described by the two-band model as well as by the anisotropic gap model. However, it was recently predicted that λ_c/λ_{ab} should increase with temperature and reach almost 1 at 0 K (clean limit) in the two-band model,[22] which is in contradiction to our results, whereas the γ(T) behavior depends on the shape of the gap in the anisotropic gap model.[4,20]

The further mixed-state parameters can be calculated

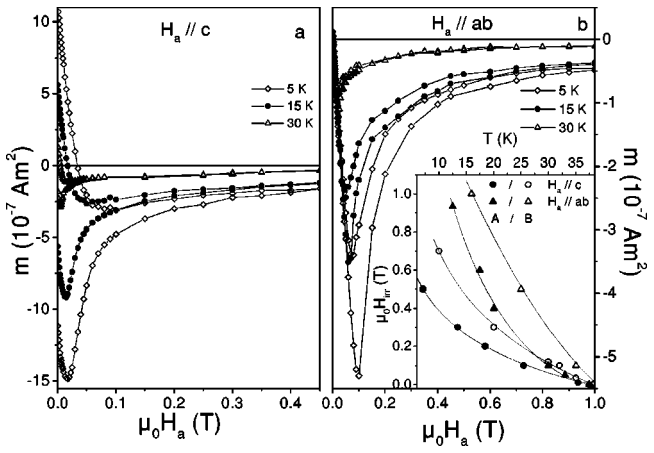

FIG. 3. Hysteresis loops of sample A for (a) $H_a \| c$ and (b) $H_a \| ab$. Inset: Irreversibility line of samples A and B for $H_a \| c$ and $H_a \| ab$.

from the London theory and some Ginzburg-Landau relations. For instance, the magnetic penetration depth in the planes (λ_{ab}) is obtained from $\partial M/\partial \ln(H_a) = \phi_0/(8\pi\lambda_{ab}^2)$ for $H_a \| c$ ($M = m_r$ per unit volume, $\phi_0 \cong 2.07 \times 10^{-15}$ V s). Since sample A shows a reversible magnetization already at very small fields (cf. Fig. 3), λ_{ab} can be evaluated in the whole temperature range from 5 K to T_c [see Fig. 2(a)]. A fit of $\lambda_{ab}^{-2}(t)$ leads to $\lambda_{ab}(0) = 82$ nm and shows that the temperature dependence lies in between the (clean limit) BCS[23] and a typical strong-coupling model[17] for $T > 20$ K. At low temperatures, however, we find a significant deviation indicating a smaller excitation energy than according to the BCS theory, in agreement with other experiments.[24,25] Again, the two-band model can describe such a scenario, but our data would suggest a rather weak influence of the band with the smaller gap. (Usually, the contributions of the two bands are simply weighted and added and the weights are used as fit parameters.[26,27]) The anisotropic gap model provides similar results.[4] Further work on more comprehensive calculations including material-dependent parameters are currently under way. The penetration depth in c direction is obtained from $\lambda_c = \gamma\lambda_{ab}$, hence $\lambda_c(0) = 370$ nm. The evaluation of λ_c from the $m(T)$ measurements for $H_a \| ab$ confirms the anisotropy, but is affected by comparatively large errors.

Further, the (GL) relation $\mu_0 H_{c2}^c = \phi_0/(2\pi\xi_{ab}^2)$ gives access to the coherence length in the a-b plane ξ_{ab} and in the c direction $\xi_c = \xi_{ab}/\gamma$ [Fig. 2(b)]. Accordingly, $\xi_{ab}(0) = 10.2$ nm and $\xi_c(0) = 2.3$ nm.

The lower critical field H_{c1} can be calculated from $\mu_0 H_{c1}^x = [\phi_0/(4\pi\delta\lambda_{ab}^2)][\ln(\delta\lambda_{ab}/\xi_{ab}) + 0.5]$ ($x = c$ and $\delta = 1$ for $H_a \| c$ and $x = ab$ and $\delta = \gamma$ for $H_a \| ab$), leading to $\mu_0 H_{c1}^c(0) = 63$ mT and $\mu_0 H_{c1}^{ab}(0) = 22$ mT [Fig. 2(c)]. A direct experimental assessment of H_{c1} is usually quite difficult, because only the penetration field H_p, i.e., the field at which the first flux lines enter the sample can be obtained, which depends on the sample geometry,[28] the anisotropy, and the pinning force.[29] We determined H_p from measurements of the trapped magnetic moment (with a resolution of better than 10^{-10} A m^2), i.e., by measuring the moment in zero field after successively applying higher external fields and searching for the first deviation from zero at H_p.[30] The effect of the geometrical barrier was numerically calculated according to Ref. 31, including a rough estimation of the influence of the anisotropy. For example, $H_{c1}^c/H_p^c \cong 17.7$ for $\gamma = 4.5$ in sample A and $\mu_0 H_{c1}^c(5\ \mathrm{K}) \cong 70$ mT, not too far away from the GL result. The geometry effects are almost negligible for $H_a \| ab$ (i.e., $H_{c1}^{ab} \cong H_p^{ab}$), which provides an excellent verification of the GL results [cf. Fig. 2(c)].

Furthermore, the thermodynamic critical field is calculated from the GL relation $\mu_0 H_c = \phi_0/(\sqrt{8}\pi\lambda_{ab}\xi_{ab})$ and found to be 0.28 T at 0 K. Because $\Delta f = \mu_0 H_c^2/2$ (condensation energy), it can also be obtained by integrating the reversible magnetization $M(H_a)$, i.e., $\Delta f = \mu_0 \int_0^{H_{c2}} M dH_a$. The reversible magnetic moment is either calculated from the irreversible branches of the magnetization in increasing (m_+) and decreasing (m_-) fields in the fully penetrated state, $m_r = (m_+ + m_-)/2$ (cf. Fig. 3) or directly measured. The results of the numerical integration are shown in Fig. 2(d) and denoted by $H_a \| c$ direct and $H_a \| ab$ direct, respectively. A comparison with the GL results indicates that the London model for the magnetic penetration depth and the GL relations for H_{c2} and ξ represent excellent solutions for MgB_2. The maximum difference at low temperatures is less than 2%. To check the influence of uncertainties near H_p in the direct evaluation (geometrical barrier, flux pinning), we replace $M(H_a)$ at 5 K by the separately measured Meissner slope at $0 \leqslant H_a \leqslant H_{c1}(1-D)$ and by a simple logarithmic behavior at $H_{c1}(1-D) \leqslant H_a \leqslant H_{c1}$, i.e., we simulate the behavior of an ellipsoidal sample, where the ''effective demagnetization factor'' D is determined from $M(H_a) = -H_a/(1-D)$ in the Meissner regime. This procedure reduces H_c at 5 K and brings the above difference to almost zero.

The deviation function $D(t) = [H_c(t)/H_c(0)] - [1-t^2]$ describing the deviation of $H_c(t)$ from the parabolic behavior (two fluid model) and indicating the coupling strength in a conventional superconductor is shown in the inset of Fig. 2(d). The maximum from -0.3% to -0.9% lies in between the weak-coupling ($\sim -3.5\%$) and the strong-coupling result ($\sim +2.5\%$ for Pb). Although we have to consider evaluation errors, the results indicate a clear deviation from the weak-coupling model, even if we consider the anisotropy (cf. Ref. 4), and is consistent with other experiments.[2,3]

The GL parameter $\kappa = \lambda/\xi$ is defined at $T = T_c$. At lower temperatures the Maki parameters[32] $\kappa_1 = H_{c2}/(\sqrt{2}H_c)$ and $\kappa_2 = [0.5 + 0.43/(\partial M/\partial H_a)_{H_{c2}} - 0.43D]^{1/2}$ can be used with $\kappa_1(T_c) = \kappa_2(T_c) = \kappa$. κ_1 ($= \lambda/\xi$ in the GL model) is shown in Fig. 2(e) for $H_a \| c$. Linear extrapolations lead to $\kappa_1^c(0) = 8.1$ and $\kappa_1^c(T_c) = 4.7$. The ratio $\kappa_1^c(0)/\kappa_1^c(T_c)$ is 1.72 and considerably larger than the BCS value (1.26 in the clean and 1.20 in the dirty limit[16]), but this is not unexpected considering stronger coupling[17] and anisotropy. κ_2 depends on the slope of M near H_{c2} and allows a precise determination of κ^c, which is again found to be 4.7 from a linear extrapolation to T_c. For $H_a \| ab$, we get $\kappa_1^{ab} = \gamma\kappa_1^c$ and therefore $\kappa_1^{ab}(0) = 37.1$ and $\kappa_1^{ab}(T_c) = 4.7$. The errors in κ_2^{ab} are relatively

TABLE I. Summary of mixed-state parameters for MgB_2.

$\mu_0 H_{c2}^c(0)$	3.18 T	$\mu_0 H_{c2}^{ab}(0)$	14.5 T	T_c	38 K
$\mu_0 H_{c1}^c(0)$	63 mT	$\mu_0 H_{c1}^{ab}(0)$	22 mT	$\mu_0 H_c(0)$	0.28 T
$\lambda_c(0)$	370 nm	$\lambda_{ab}(0)$	82 nm	$\gamma(0)$	4.6
$\xi_c(0)$	2.3 nm	$\xi_{ab}(0)$	10.2 nm	$\gamma(T_c)$	1
$\kappa_1^c(0)$	8.1	$\kappa_1^{ab}(0)$	37.1	$\kappa(T_c)$	4.7

large in this case because of the very small slope of the magnetization near H_{c2}, but the extrapolation leads to $\kappa^{ab}=5$, very close to κ^c.

At last, we turn to the irreversible properties of the MgB_2 single crystals. Hysteresis curves recorded at different temperatures are presented in Fig. 3 for $H_a \| c$ and $H_a \| ab$. They demonstrate the excellent crystal quality by the small hysteresis and the low irreversibility fields in both directions. Note that all data points presented in Fig. 3 were measured in the fully penetrated state. According to the Bean model[33] (J_c is assumed to be constant), the critical current density in the planes can be calculated from the irreversible magnetic moment ($m_i=[m_+-m_-]/2$). For rectangular samples we use $J_c(B)=\{m_i(B)/\Omega\}\{4/[b(1-b/3a)]\}$ (sample volume: $\Omega=abc$), and get 1.4×10^9 Am^{-2} at 5 K in the remnant state for both samples. To obtain the irreversibility line, the onsets of a difference between the field-cooled and the zero-field-cooled $m(T)$ measurement were evaluated. The results of Fig. 3 (inset) show that the irreversibility line is very low for both field directions.

In summary, we presented measurements of the magnetic moments in single crystalline MgB_2 for fields $H_a \| c$ and $H_a \| ab$, and the subsequent evaluation of the basic mixed-state parameters. The most important results are summarized in Table I. The general consistency of the data set that is documented in a presentable form, e.g., by the results on the thermodynamic critical field, suggests that the standard theoretical description can be employed in MgB_2. The data indicate that MgB_2 is a low-κ type-II superconductor in the clean limit with an intermediate electron phonon coupling strength (cf. also Refs. 34 and 35), but a very large anisotropy.

We wish to thank F. M. Sauerzopf for useful discussions and H. Hartmann for technical assistance. This work was supported in part by the Austrian Science Foundation (FWF Project No. 14422), the Austrian Exchange Service (OEAD Grant No. 27/2000), the European Commission (program Grant No. ICA1-CT-2000-70018, Center of Excellence CELDIS), the TMR Network SUPERCURRENT, and the Swiss National Science Foundation.

*Electronic address: zehetm@ati.ac.at

[1] J. Nagamatsu *et al.*, Nature (London) **410**, 63 (2001).
[2] S.L. Bud'ko *et al.*, Phys. Rev. Lett. **86**, 1877 (2001).
[3] J.W. Quilty *et al.*, Phys. Rev. Lett. **88**, 087001 (2002).
[4] S. Haas and K. Maki, Phys. Rev. B **65**, 020502 (2001).
[5] S.V. Shulga *et al.*, cond-mat/0103154 (unpublished).
[6] S. Lee *et al.*, J. Phys. Soc. Jpn. **70**, 2255 (2001).
[7] A.K. Pradhan *et al.*, Phys. Rev. B **64**, 212509 (2001).
[8] Yu. Eltsev *et al.*, Phys. Rev. B **65**, 140501(R) (2002).
[9] F. Manzano *et al.*, Phys. Rev. Lett. **88**, 047002 (2002).
[10] M. Angst *et al.*, Phys. Rev. Lett. **88**, 167004 (2002).
[11] A.V. Sologubenko *et al.*, Phys. Rev. B **65**, 180505(R) (2002).
[12] U. Welp *et al.*, cond-mat/0203337 (unpublished).
[13] J. Karpinski *et al.*, cond-mat/0207263 (unpublished).
[14] M.A. Angadi *et al.*, Physica C **177**, 479 (1991).
[15] F.M. Sauerzopf, Phys. Rev. B **57**, 10 959 (1998).
[16] E. Helfand and N.R. Werthamer, Phys. Rev. **147**, 288 (1966).
[17] J.P. Carbotte, Rev. Mod. Phys. **62**, 1027 (1990).
[18] W. Pitscheneder and E. Schachinger, Phys. Rev. B **47**, 3300 (1992).
[19] H.W. Weber *et al.*, Phys. Rev. B **44**, 7585 (1991).
[20] A.I. Posazhennikova, T. Dahm, and K. Maki, cond-mat/0204272 (unpublished).
[21] D. Zech *et al.*, Phys. Rev. B **54**, 12 535 (1996).
[22] A.A. Golubov *et al.*, cond-mat/0205154 (unpublished).
[23] B. Mühlschlegel, Z. Phys. **155**, 313 (1959).
[24] F. Giubileo *et al.*, Phys. Rev. Lett. **87**, 177008 (2001).
[25] P. Szabó *et al.*, Phys. Rev. Lett. **87**, 137005 (2001).
[26] C.P. Moca, Phys. Rev. B **65**, 132509 (2002).
[27] F. Bouquet *et al.*, Europhys. Lett. **56**, 856 (2001).
[28] E. Zeldov *et al.*, Phys. Rev. Lett. **73**, 1428 (1994).
[29] A.V. Kuznetsov, D.V. Eremenko, and V.N. Trofimov, Phys. Rev. B **56**, 9064 (1997).
[30] C. Böhmer, G. Brandstätter, and H.W. Weber, Supercond. Sci. Technol. **10**, A1 (1997).
[31] T.B. Doyle, R. Labusch, and R.A. Doyle, Physica C **290**, 148 (1997).
[32] K. Maki, Physics (Long Island City, N.Y.) **1**, 21 (1964).
[33] C.P. Bean, Phys. Rev. Lett. **8**, 250 (1962).
[34] H.J. Choi *et al.*, cond-mat/0111182 (unpublished).
[35] H.J. Choi *et al.*, cond-mat/0111183 (unpublished).